Text S1. Electronic Supplementary Figures

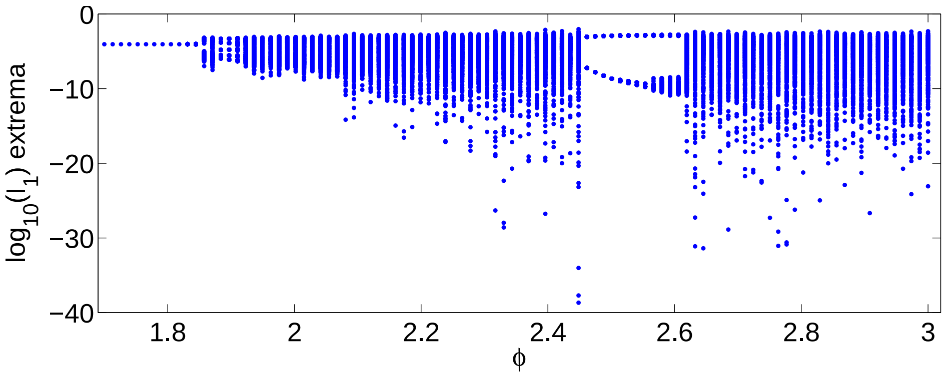

Figure S1: Extrema of the infected classes for fully symmetric serotype parameters (in log base 10 scale). The system in eq. (1) of the supplementary text has a Hopf bifurcation at $\phi \approx 1.85$ and asymptotically tends to oscillate periodically when $1.85 \lesssim \phi \lesssim 1.93$. For higher values of the ADE factor,the dynamics are mostly chaotic with the exception of narrow windows where stable orbits exist, such as the one in the interval $2.45 \lesssim \phi \lesssim 2.55$.

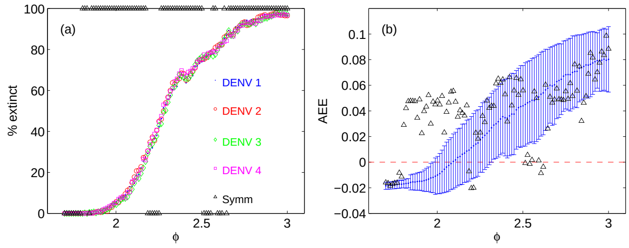

Figure S2: Plot of the ADE factor vs. proportion of runs that have minima of the infected classes below a threshold of 10^{-7} (a). Plot of the AEE (see text) at each value of the ADE factor; the errorbars indicate one standard deviation over the 400 runs (b). The black markers indicate the strictly serotype-symmetric situation. For each run, the transmission rates are distributed as $\beta_i = \beta_0 + \sigma_\beta \cdot \mathcal{N}(0,1)$ with $\sigma_\beta = 75$. Here, $\beta_0 = 300$. The values of the birth/death rates, duration of the incubation period and recovery rate are as in Table A.1.

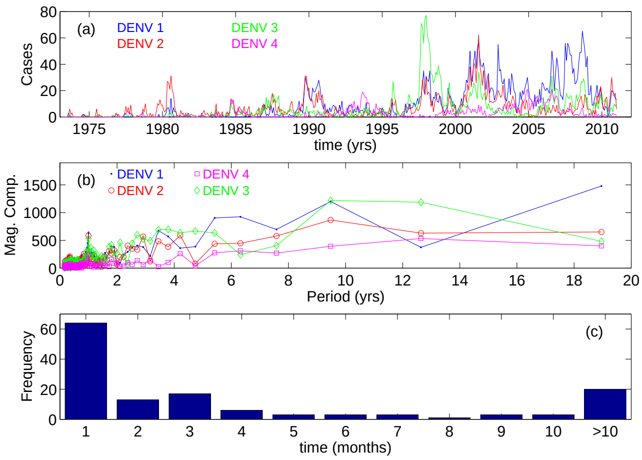

Figure S3: Panel (a): time series of the four dengue serotypes in Bangkok, 1973-2010. Panel (b): magnitude of the Fourier components of the time series in (a). Panel (c): histogram of the number of consecutive months without extinctions accumulated for the four serotypes. Data is from Nisalak, A., Endy, T., Nimmannitya, S., et al., 2003. *Am. J.Trop.Med.Hyg.* 68 and from Nisalak, personal communication, 2010.

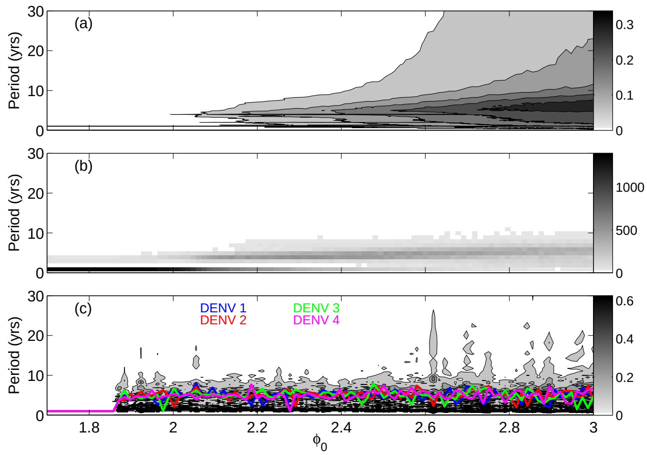

Figure S4: Panel (a): Contour plot of the magnitudes of the Fourier components of the infecteds $I_i(t)$, as a function of the ADE factor ϕ, averaged over 400 runs and over the 4 strains (time series of strains that go extinct over the whole interval $1.7 \leq \phi \leq 3.0$ are removed). Panel (b): histogram of the dominant Fourier component (with the exception of the zero frequency component) of the same runs as in (a). Panel (c): same as in (a) except that only the symmetric case $\beta_i = 500$ is considered. The single dominant component for each serotype is shown with the continuous lines. In these studies, seasonality is included by taking $\beta_i \to \beta_i(1 + 0.05\cos(2\pi t))$. The values of the birth/death rates, duration of the incubation period and recovery rate are as in Table A.1.

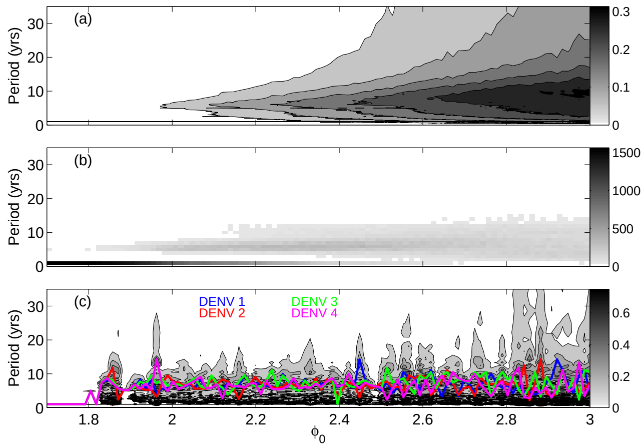

Figure S5: Panel (a): Contour plot of the magnitudes of the Fourier components of the infecteds $I_i(t)$, as a function of the ADE factor ϕ, averaged over 400 runs and over the 4 strains (time series of strains that go extinct over the whole interval $1.7 \leq \phi \leq 3.0$ are removed). Panel (b): histogram of the dominant Fourier component (with the exception of the zero frequency component) of the same runs as in (a). Panel (c): same as in (a) except that only the symmetric case $\beta_i = 300$ is considered. The single dominant component for each serotype is shown with the continuous lines. In these studies, seasonality is included by taking $\beta_i \to \beta_i(1 + 0.05\cos(2\pi t))$. The values of the birth/death rates, duration of the incubation period and recovery rate are as in Table A.1.

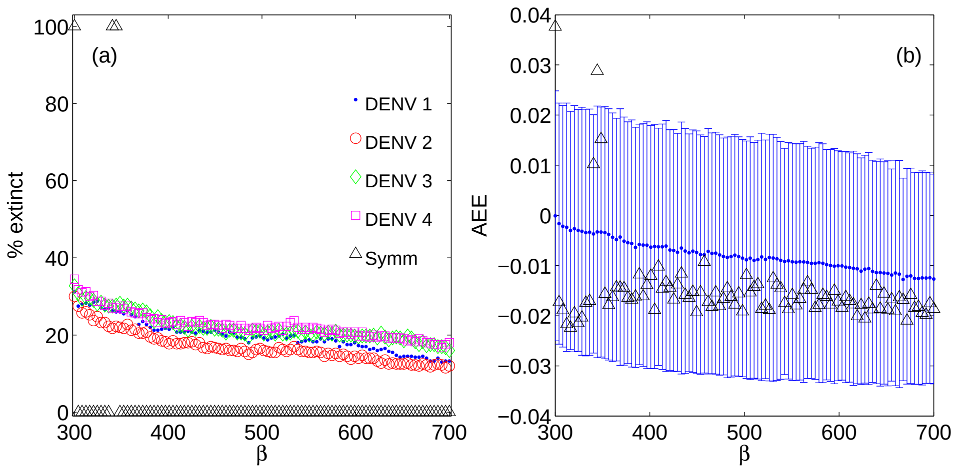

Figure S6: Proportion of runs that have minima of the infected classes below a threshold of 10^{-7} (a) and Average Expansion Exponent (b) vs. the transmission rate factor. For each run, the ADE factors are distributed as $\phi_i = \phi_0 + \sigma_\phi \cdot \mathcal{N}(0, 1)$ with $\phi_0 = 1.8$ and $\sigma_\phi = 0.4$.

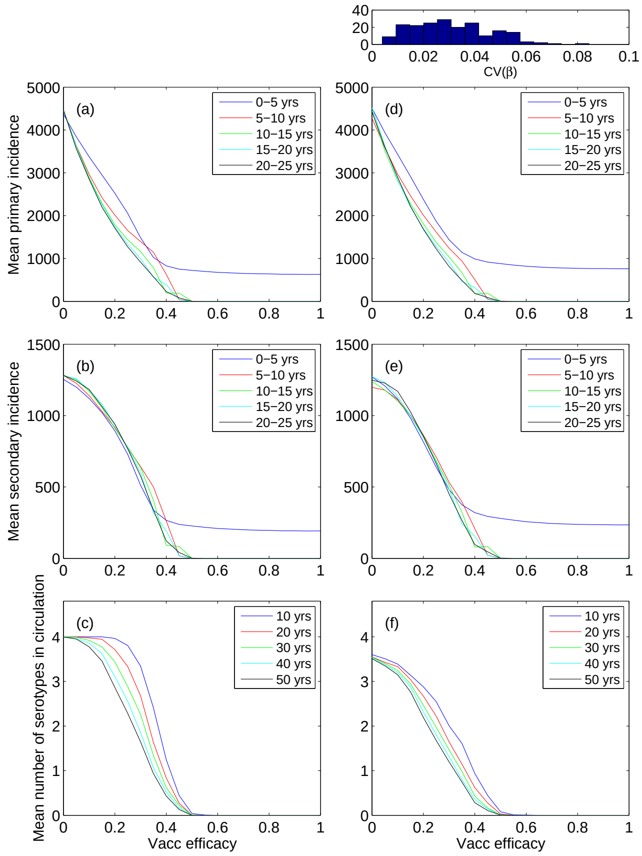

Figure S7: Time average of the primary (a and d) and secondary (b and e) incidences over the time periods indicated in each panel; and mean number of serotypes co-circulating after the time period indicated (c and f), for different values of the serotype-independent vaccine efficacy. The results in each column were obtained with 200 stochastic simulations at each value of the vaccine efficacy. The left column corresponds to symmetric transmission rates, while the column on the right corresponds to asymmetric ones. The histogram above panel (d) shows the distribution of the coefficient of variation of the four transmission rates over the 200 runs. Here, $\phi = 1.0$.

Text S2. Quantifying the Strength of the Chaotic Dynamics

One quantitative method for identifying chaotic dynamics in a system of ordinary differential equations (ODEs) is by measuring its Lyapunov exponents. The Lyapunov exponents of a dynamical system statistically quantify how rapidly neighboring points in phase space diverge or converge as time tends to infinity (see Guckenheimer, J. and Holmes, P., 1986). A positive Lyapunov exponent means that neighboring initial conditions diverge exponentially and implies the presence of chaos. In numerical computations, one calculates instead the Finite Time Lyapunov Exponents (FTLEs). As their name suggests, the FTLEs quantify the exponential separation of neighboring phase space points during finite times into the future. Computing the FTLEs relies on measuring the exponential rates of expansion and contraction produced by the ODE flow along a set of orthonormal basis vectors. It requires solving the so-called variational equations in addition to the original ODE system. An ODE system of n equations has n^2 variational equations; hence, one must solve $n(n+1)$ differential equations in total.

In contrast to the rigorous methodology described above, for this work we used a simplified algorithm to decide whether the behavior of the system is chaotic or not. This simplified approach will not give the exact same results as the method described above; however, it is computationally much more efficient and gives satisfactory results given our objectives. It relies on calculating what we call the Averaged Expansion Exponent (AEE). Given a system of n ODEs $\dot{\mathbf{y}} = F(\mathbf{y})$, we obtain the AEE as follows. First we numerically simulate the system for a statistically long time T_{trans} to allow transient dynamics to decay. Then, from the state of the system at this time $\mathbf{y}(T_{\text{trans}})$ we generate a perturbed initial condition $\mathbf{y}^{\text{pert}}(T_{\text{trans}})$ in a random direction that has components $y_i^{\text{pert}}(T_{\text{trans}}) = (1+\epsilon\mathcal{N}(0,1))\cdot y_i(T_{\text{trans}})$, for $i = 1, 2, \ldots n$. Here, $\epsilon \ll 1$ and $\mathcal{N}(0,1)$ is a Gaussian random variable with mean of zero and variance equal to one. We then numerically simulate the two copies of the system for a period of time T_{AEE}, using the initial conditions $\mathbf{y}(T_{\text{trans}})$ and $\mathbf{y}^{\text{pert}}(T_{\text{trans}})$, respectively.

A first expansion exponent is obtained by measuring the rate of exponential separation of extrema between the two copies of the system: $\lambda_1 = \frac{\log(d_{\text{first}}/d_{\text{last}})}{T_{AEE}}$, where d_{first} is the Euclidian distance between the first extrema of the original system and the first extrema of the perturbed system. To be clear, $d_{\text{first}} = |\mathbf{y}(t^*) - \mathbf{y}^{\text{pert}}(t^{**})|$ where t^* is the time of the first extrema of the original system encountered after T_{trans} and t^{**} is the time of the first extrema of the perturbed system ($|\cdot|$ is the Euclidian norm in $\mathbb{R}^n$). Analogously, d_{last} is the distance between the last extrema of the two copies of the system. By considering the separation between the extrema of the two systems instead of arbitrary points, we ensure that the rate of exponential separation is negative when the two system copies are on the same periodic orbit but are simply out of phase. We repeat the process 10 times by generating perturbed initial conditions as above at the succeeding times $T_{\text{trans}} + j \cdot T_{\text{AEE}}$, $j = 1, 2, \ldots 9$, and obtain another nine expansion exponents $\lambda_2, \ldots \lambda_{10}$. The AEE is finally obtained by averaging the ten rates of exponential expansion: $\text{AEE} = \frac{1}{10}\sum_{i=1}^{10} \lambda_i$.

The times T_{trans}, T_{AEE} and the parameter ϵ must be chosen appropriately from the dynamical time-scales of the system. After numerous tests, we selected $T_{\text{trans}} = 1000$, $T_{AEE} = 100$ and $\epsilon = 10^{-5}$.

Text S3. Persistence Studies and Vaccination

Here, we discuss the results shown in Figs. A.4 in the main text and S7 in the supplement in light of our previous serotype persistence discussions. We note that the extinction of serotypes at $\phi = 1.0$ is faster in the asymmetric case than in the symmetric one (Figs. S7c and S7f). The results at $v_{\text{eff}} = 0$ are consistent with the probabilities of persistence shown in Figs. A.1 and A.2. Comparing Figs. S7c and S7f with A.4c and A.4f, it is clear that at low vaccine efficacies, an increase of the ADE factor from 1.0 to 1.7 is detrimental to the persistence of symmetric serotypes but beneficial to the persistence of asymmetric ones. This agrees with our conclusions from Figs. A.1 and A.2, where a value around $\phi = 1.7$ was seen to be optimal for the persistence of asymmetric serotypes.